This article has been accepted for publication in a future issue of this journal, but has not been fully edited. Content may change prior to final publication. Citation information: DOI 10.1109/TPWRD.2016.2524677, IEEE Transactions on Power Delivery

Damping of VFTO in Gas-Insulated Switchgear by a New Coating Material

Marcin Szewczyk, *Senior Member, IEEE*, Wojciech Piasecki, *Member, IEEE,* Mariusz Stosur, Marek Florkowski, *Senior Member, IEEE*, Uwe Riechert, *Member, IEEE*

***Abstract*— Several methods of attenuation of Very Fast Transient Overvoltages (VFTO) in Gas-Insulated Switchgear (GIS) are under development. An approach that is currently gaining high attention among researchers is based on the application of magnetic cores dissipating the energy associated with VFTO due to eddy current losses and magnetic hysteresis losses. This paper presents an advancement in this approach, by introducing a new material type (denoted in the present paper as "nanoflakes"). This new material comprises macro pieces of nanocrystalline ribbons (with the size ranged in square millimeters), acquired from crumbled nanocrystalline cores of a standard design. The material is characterized by relatively high magnetic permeability, poor electrical conductivity, and high saturation flux level. The material is suitable for application as a coating layer applied to the surfaces of an inner and/or an outer GIS conductor, as a fill-in material in the GIS shielding elements, or as a standard shaped core. The paper presents the material major features, outlines its development process, and reports on validation of the material effectiveness in real VFTO conditions. The validation is based on the measurement of VFTO attenuation in full-scale 550 kV GIS test set-up.**

***Index Terms*— Very Fast Transient Overvoltages (VFTO), Gas-Insulated Switchgear (GIS), disconnector switch, magnetic material, magnetic ribbon, attenuation, damping, transients, switching**

I. Introduction

A. Very Fast Transient Overvoltages in GIS

LARGE AC power grids are backboned with high power capacity corridors rated at high- (HV) and ultra-high voltage (UHV) levels to maintain power transmission losses at acceptable limits. The IEC ratio between the rated voltages and the withstand voltage levels declines towards higher rated voltages. For Gas-Insulated Switchgear (GIS), Very Fast Transient Overvoltages (VFTO) are generated by operations of disconnectors. With the VFTO peak values which remain independent of the rated voltages [1], [2], for the rated voltages exceeding 500 kV the VFTO can be as high as the IEC withstand voltage levels. Hence, for HV and UHV GIS the VFTO is carefully examined by the GIS designers in order to assess the safety margins of the equipment. According to particular design selection, a decision on application of the VFTO mitigation solution is being made in order to ensure the required robustness of the equipment.

B. Methods on VFTO Attenuation

Several methods on VFTO attenuation are known, as thoroughly reviewed in [3], [4]. In [5] an overview is given of the methods based on the application of magnetic cores. The latter methods involve commercially available magnetic cores of different types, sizes, and material properties: ferrite [6], amorphous [7], nanocrystalline [5]. The cores are wound on the inner conductor of the GIS busbar and located under an electric field control element. The number and the dimensions of the cores are selected according to the required attenuation effect.

Dominant physical mechanisms responsible for the VFTO attenuation in the magnetic cores include eddy current and magnetic hysteresis losses [7], [8]. These mechanisms are highly frequency dependent and are affected by the magnetic saturation effect of the material [7], [8]. In [5], [7], [9] the Authors show comparison of commercially available magnetic cores of different types, indicating that the attenuation factor is highly dependent on physical properties of the magnetic material and on the number of the magnetic cores involved.

Parameters of the cores strongly depend on the frequency [5] and the current [8] associated with the VFTO conditions. The required number of the cores of a given type and dimensions is evaluated experimentally [5], [7] and numerically [7], [8] in order to achieve the required VFTO attenuation effect. Flexibility of the selected material in terms of its manufacturing for the required size selection is a key factor in order to achieve an optimized design for the required VFTO damping effect, the GIS dielectric design, the GIS thermal and mechanical performance.

C. Paper Overview

In this paper, we present a new magnetic material (nanoflakes), developed and tested for VFTO attenuation in GIS. Section I gives background information and main references that contain throughout overview of the state-of-the art methods on VFTO attenuation in GIS based on application of magnetic materials. Section II presents the nanoflakes material itself, its main features, and initial low voltage tests. Outline of the material development process is also given. Section III provides description of the full-scale 550 kV GIS test set-up used for experimental evaluation of the nanoflakes

M. Szewczyk, W. Piasecki, M. Stosur, M. Florkowski are with ABB Corporate Research Center, 31-038 Krakow, Starowislna 13A, Poland (e-mail: marcin.szewczyk@pl.abb.com, mariusz.stosur@pl.abb.com, wojciech.piasecki @pl.abb.com, marek.florkowski@pl.abb.com).

U. Riechert is with ABB Switzerland Ltd., Zürich 8050, Switzerland (e-mail: uwe.riechert@ch.abb.com).

Corresponding author: M. Szewczyk (e-mail: marcin.szewczyk@pl.abb.com).

Color versions of one or more of the figures in this paper are available online at http://ieeexplore.ieee.org

This article has been accepted for publication in a future issue of this journal, but has not been fully edited. Content may change prior to final publication. Citation information: DOI 10.1109/TPWRD.2016.2524677, IEEE Transactions on Power Delivery

material effectiveness. Section IV reports on the measurement results conducted in the 550 kV test set-up introduced in Section III. Section V presents discussion on the measurement results, and offers conclusions.

II. Nanoflakes: New material for VFTO Damping in GIS

A. Material Description

The nanoflakes material is composed of an elastomer matrix filled with a resistive inset, in which macro pieces of crumbled nanocrystalline ribbons are suspended. The pieces of the nanocrystalline material are acquired from the commercially available magnetic cores (e.g. [10]).

Selection of the nanocrystalline ribbons for development of the new material was motivated by the fact that the nanocrystalline cores have experimentally proven their effectiveness for damping of VFTO in GIS, as reported in e.g. [11]. The nanocrystalline cores are characterized with high magnetic permeability and high saturation level as compare to the ferrite rings tested in e.g. [6].

As compared to the standard nanocrystalline cores, the new material is characterized with the resistive distributed gap introduced in between the nanocrystalline pieces. This implies decreased magnetic permeability. In the material comprising a dielectric matrix the eddy currents can circulate only within the nanocrystalline pieces. However, if the material is additionally filled with a resistive particles, the parameters of the material can be adjusted by the density of the nanocrystalline pieces, their sizes, and also by the resistivity of the matrix. This resistivity can be adjusted by an addition of appropriate amount of carbon powder filler.

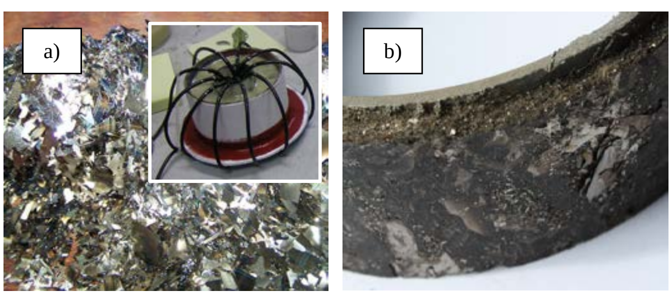

Fig. 1 Crushed nanocrystalline material (a), inset: magnetic core formed with crushed nanocrystalline material submersed in resin for current treatment and inductance measurement; example of manufactured nanoflakes coating (b).

Fig. 1a shows an example of the crushed nanocrystalline material used for the development of the nanoflakes material shown in Fig. 1b.

The new material involves the manufacturing process that offers high degree of flexibility in terms of the geometry design, which further gives an opportunity for optimization of the magnetic coating dimensions and shape. The material can be shaped to form a coating layer to the surfaces of the inner and/or the outer GIS conductors, to be placed inside shielding elements, or to form a ring-shaped magnetic cores.

B. Material Preparation and Initial Measurements

In order to perform an initial evaluation of the material, samples in a form of toroidal cores were prepared. The processing of the material was performed under the DC magnetic field so that the effect of the nanoflakes orientation within the material could also be controlled. The crumbled nanocrystalline ribbons shown in Fig. 1a were mixed with a polymer matrix (resin) and placed in a toroidal form (see inset in Fig. 1a), on which a winding comprising of 10 turns of wire was wound. The nanocrystalline pieces were pre-treated with a DC current so that the associated magnetic flux aligned the pieces in the resin according to the minimum energy condition.

TABLE I
Low voltage measurement results: I, t – current and time for pre-treatment, L – measured inductance, δL – inductance gain in reference to zero-current inductance ($L_0 = 0.015$ mH)

I [A]	t [minutes]	L [µH]	δL [%]
0	0	15	0
10	1	15	0
20	1	20	33
20	40	25	67

After the pre-treatment, the DC current was switched off and the inductance was measured. Due to the high viscosity of the resin the relaxation time of the nanocrystalline pieces was long enough so there was no significant change in the pieces orientation between the pre-treatment and the inductance measurement. The inductance was measured for two DC pre-treatment current values (10 A and 20 A) and for two pre-treatment times (1 minute and 40 minutes).

Results of this experiment are shown in Table I. For the case with the DC current of 20 A applied for 40 minutes, an inductance increase by 67% was observed as compared to the reference case.

Based on these results a full-scale 550 kV GIS conductor was developed, as shown in Section III.

III. Full-scale HV Experimental Set-up at 550 kV

A. GIS Test Set-up Arrangement

Fig. 2 shows the test set-up introduced in [11] and used in the measurements reported in the present paper. High voltage impulse generator was used to supply Lightning Impulse (LI) voltage $1.2/50\ \mu s$ to the AIS-GIS bushing. The test set-up comprised a spark-gap compartment filled with SF_6 gas (see Fig. 2a, the component marked with red color). The gap distance and the SF_6 gas pressure were controlled during the measurements to provide voltage breakdown at required instantaneous value of the LI voltage. The spark gap of 10 mm with 0.4 MPa pressure of SF_6 gas was used to initiate the breakdown at 500 kV of LI voltage. By lowering the SF_6 gas pressure to 0.1 MPa, the breakdown voltage decreased to 200 kV was used in addition to 500 kV voltage. Each breakdown in SF_6 spark gap initiated VFTO propagation in the GIS components. Air-insulated busbar compartments were used for inserting the VFTO mitigation solutions under the test (i.e. the magnetic cores and the new nanoflakes material), as shown in Fig. 2 (see Fig. 2a, the components marked with grey color). The GIS test set-up was dismounted and mounted between any changes in the material under test. Air insulation used in the bus-bar compartment significantly reduced the time needed for the set-up re-arrangement.

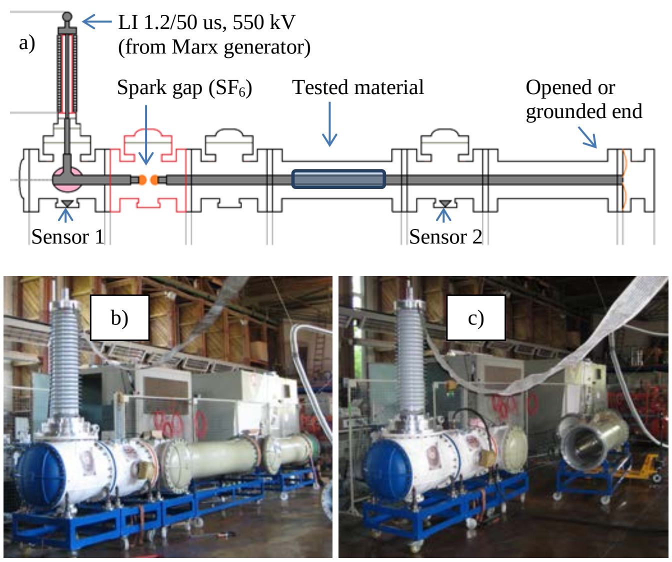

Fig. 2 Measurement set-up of 550 kV GIS [5, 11] with sensors indicated (a), GIS components: mounted (b) and dismounted (c); Marx generator provides 1.2/50 μs impulse voltage to SF_6 spark gap compartment; GIS components filled with SF_6 gas / air are marked with red / grey color in (a).

B. Overall Voltage Waveforms

Voltage waveforms were measured with high frequency capacitive sensors located in dedicated GIS compartments according to Fig. 2.

Fig. 3 shows example of the overall voltage waveforms recorded for the GIS with open end, with Sensor 1 and Sensor 2. First breakdown (followed by the VFTO) occurs in the spark gap with SF_6 gas. After the voltage builds up in the whole GIS set-up, second breakdown occurs in an air insulated bus-duct. This is due to the lowered insulation withstand voltage for the air-insulated compartment being originally designed for operation when filled with SF_6 gas.

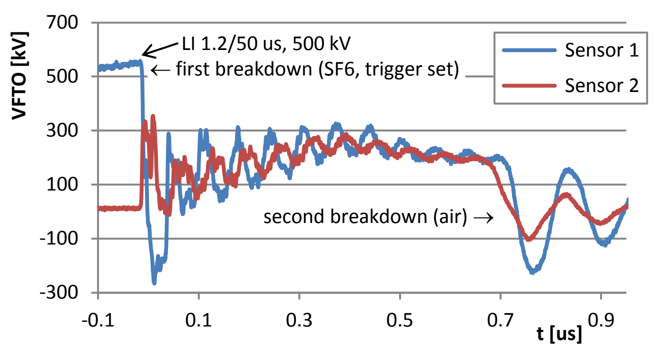

Fig. 3 Voltage waveforms recorded with Sensor 1 and Sensor 2 (see Fig. 2); indicated are: LI voltage 1.2/50 μs, first breakdown (in SF_6, trigger set), second breakdown (in air), open end.

It can be seen in Fig. 3 that after the first breakdown occurrence, the voltages recorded by both sensors build-up according to the capacitor loading curve. After the second breakdown (occurring in the end of the GIS), the voltages oscillate with half-frequency around the zero voltage level (as the set-up is grounded by the flashover).

For the shots with the grounded end, grounded copper stripe was connected between conductor and enclosure at the right-hand end of the set-up (see Fig. 2). Main frequencies of the VFTO waveforms, as associated with the overall GIS test set-up length, are: 15 MHz for the open end, and 7.5 MHz for the grounded end.

C. Measuring Sequence

Reference voltage waveforms (without magnetic material) were recorded before and after measurements. Fig. 4 shows their mutual good agreement for the example of test with open end.

For each study case (i.e. each arrangement of the test set-up and of the attenuation material used), the voltage waveforms were measured for several tests. The averaged waveforms of several tests were then analyzed, as reported in Section IV. Since the triggering was set on the falling slope of the first breakdown (see Fig. 3, Sensor 1), the waveforms recorded were not affected by the averaging procedure.

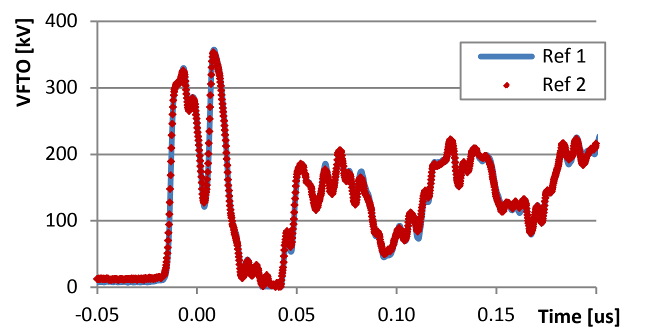

Fig. 4 Voltage waveforms measured with Sensor 2 (as per Fig. 2); before (Ref 1, line) and after (Ref 2, dots) all measurements (for the GIS open end).

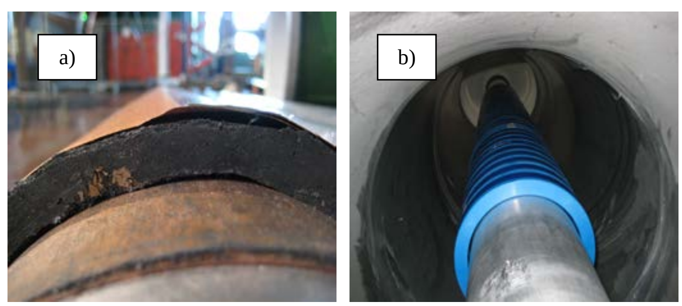

Fig. 5 Example of 550 kV GIS conductor with nanoflakes material (a) and with standard magnetic cores (b).

D. Tested Magnetic Materials: Nanoflakes and Standard Cores

Fig. 5 shows an example of 550 kV GIS conductor with the new nanoflakes material (Fig. 5a) and with the standard magnetic cores (Fig. 5b).

The nanoflakes material shown in Fig. 5a was built with the nanocrystalline ribbons of the same type as used in the standard cores shown in Fig. 5b selected for testing. The ribbons were crumbled to the extent that the approximate size of the pieces was in the millimeter size range. The maximum size of the pieces in the representative sample was not exceeding 12 mm in the longest direction. As the elastomer matrix a polyurethane material was used. As the carbon powder, a graphite material was used, with the grain size in the range between 0.1 mm to 1 mm. For the nanoflakes

This article has been accepted for publication in a future issue of this journal, but has not been fully edited. Content may change prior to final publication. Citation information: DOI 10.1109/TPWRD.2016.2524677, IEEE Transactions on Power Delivery

material under test, commercially available nanocrystalline iron based material was used. The GIS conductor was covered with an insulating lacquer, on which the material was applied.

Fig. 6 illustrates the manufacturing process. During the process, the GIS conductor was positioned vertically (see Fig. 6a). A magnetizer shown in Fig. 6b was inserted into the GIS conductor in Fig. 6a and supplied with a DC current to produce the magnetic field around the GIS conductor. The nanoflakes material according to the description given above was poured (in the form of a liquid) to the forming element. This constituted a segment of the nanoflakes material of few centimeters width. Within the segment, the nanocrystalline ribbons were orientated along the surface of the GIS conductor according to the magnetic flux generated by the magnetizer. After drying of the segment, the magnetizer was moved to the next position, where the process was repeated. Ensuring repeatable material properties in a potential product would require a stable manufacturing process, in which resistivity of the material as well as size distribution and density of the nanocrystalline pieces are under appropriate control.

Fig. 6 GIS conductor with nanoflakes material in the forming element, b) magnetizer used inside the GIS conductor, supplied with a DC current to generate magnetic field around the GIS conductor for orientating the ribbons along the GIS conductor surface.

The material was manufactured with the same thickness as the standard cores used in the measurements. Semiconductive paper was used as an outer layer, connected at one side to the GIS conductor, to provide shielding that allowed to avoid local gradients of electric field.

The nanoflakes material selected for testing had the same thickness as of the cores, and the length adjusted to provide similar attenuation as compare to the 8 cores employed. Also, same nanocrystalline ribbons were used as in the nanoflakes material as in the tested standard cores.

IV. Measurement Results

Measurements were conducted in the test set-up shown in Fig. 2 for the two magnetic materials shown in Fig. 5. Two breakdown voltage levels were employed: 500 kV and 200 kV, with 0.4 MPa and 0.1 MPa pressure of SF_6 gas in the spark gap compartment respectively. For each breakdown voltage level, the voltage waveforms were recorded with two sensors shown in Fig. 2, for two VFTO frequency conditions.

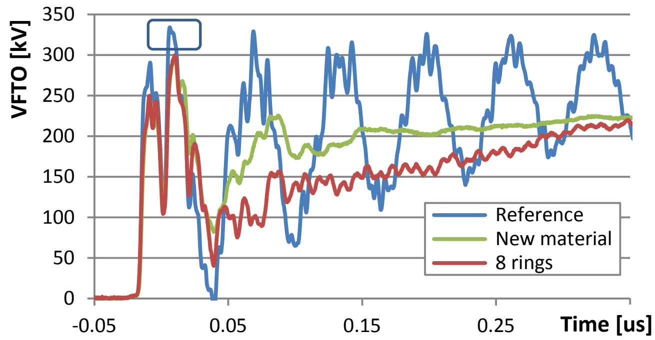

Fig. 7 Measurement results: VFTO voltage waveforms for different magnetic materials; for 500 kV, GIS with **open end**, Sensor 2; global maximum marked.

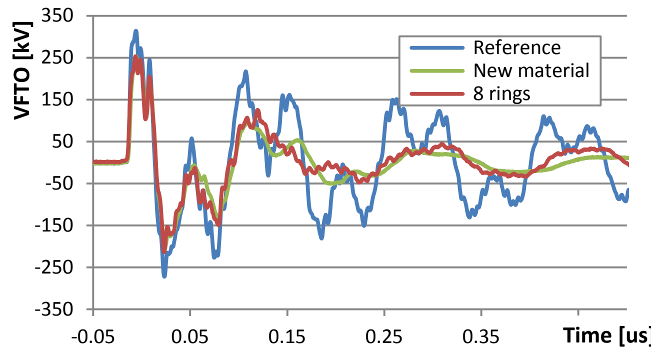

Fig. 8 Measurement results: VFTO voltage waveforms for different magnetic materials; for 500 kV, GIS with **grounded end**, Sensor 2.

Fig. 7-10 show examples of the voltage waveforms recorded by Sensor 2 for 500 kV breakdown voltage, for open and grounded end conditions. Table II shows attenuation factors for each measured case shown in Fig. 7-10. The attenuation factor was defined as [5]:

$$\frac{u_{\mathrm{ref}}^{max} - u^{max}}{u_{\mathrm{ref}}^{max}} \times 100\%, \quad (1)$$

where *max* means global VFTO maximum (first peak), for the voltage waveform u^{max} obtained with the magnetic material involved, and for the reference waveform u_{ref}^{max} obtained without the magnetic material. As an example, the global maximum of the VFTO waveform is marked in Fig. 7.

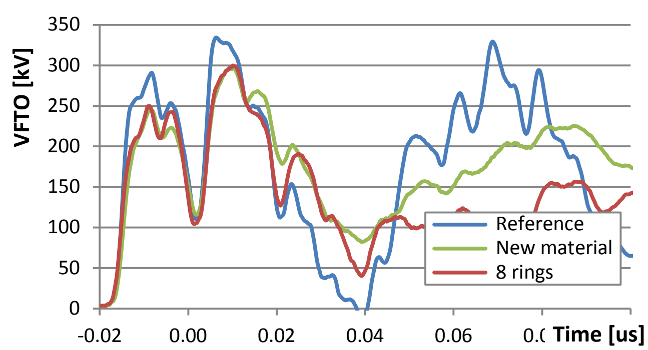

Fig. 9 Measurement results shown in **Fig. 7** zoomed to show first peak attenuation; VFTO waveforms for 500 kV, GIS with **open end**, Sensor 2.

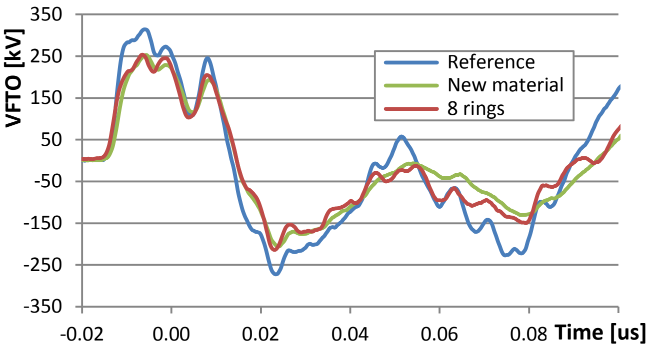

Fig. 10 Measurement results shown in **Fig. 8** zoomed to show first peak attenuation; VFTO waveforms for 500 kV, GIS with **grounded end**, Sensor 2.

In addition to the measurements conducted for the breakdown voltage of 500 kV, as shown in Fig. 7-10 and Table II, for the new nanoflakes material the measurements were conducted also for 200 kV (for the two frequency conditions: 15 MHz and 7.5 MHz). As compared to the 500 kV results summarized in Table II, the 200 kV attenuation increased from 11.2% to 13.7% for 15 MHz, and from 19.1% to 23.3% for 7.5 MHz (i.e. by 22.3% and 22.0% respectively).

TABLE II
VFTO attenuation (first peak) for new nanoflakes material and for 8 cores, as shown in Fig. 7-10; for 500 kV and two frequency conditions (15 MHz and 7.5 MHz)

VFTO conditions	**VFTO attenuation [%]**	
	Nanoflakes	**8 cores**
500 kV, 15 MHz	11.2	10.3
500 kV, 7.5 MHz	19.1	19.5

V. Conclusions

A novel magnetic material, called nanoflakes, has been introduced for application of VFTO attenuation in GIS. The material relies on crumbled nanocrystalline ribbons located in a resistive filler.

Full-scale VFTO measurements were performed in 550 kV experimental set-up, for two options of VFTO attenuation solutions: the new nanoflakes material, and the standard nanocrystalline cores. Number of magnetic cores and dimensions of the nanoflakes material were selected in order to obtain similar attenuation of both solutions. Attenuation factor was measured for two GIS arrangements, with open and grounded end, characterized in different VFTO main frequency components: 15 MHz and 7.5 MHz respectively.

For the most severe conditions (500 kV, 15 MHz), both solutions provided more than 10% of the VFTO first peak attenuation. Even higher attenuation was observed for next peaks damping. Higher attenuation was also observed for lower frequency (7.5 MHz) and for lower voltage (200 kV).

To achieve same attenuation, the new material requires 60% more overall material (in terms of weight) than the standard cores. The manufacturing process involved for production of the new material offers high degree of flexibility in terms of the geometry design, which further gives an opportunity for optimization of the magnetic material dimensions and shape. The material can be shaped to form a coating layer to the surfaces of the inner and/or the outer GIS conductors, to be placed inside shielding elements, or to form a ring-shaped magnetic cores. Placing a magnetic-resistive material of any kind (such as magnetic cores or nanoflakes material) on the GIS bus-bar conductor will modify the dielectric distance between the main conductor and the enclosure, thus will reduce the insulation strength. This needs to be taken into account in the dielectric design of the GIS busbar.

This experimental work can serve as a base for modeling work and analysis of physical characteristics of the new material in high frequency and high current VFTO conditions.

VI. Acknowledgment

Experimental part of this work was conducted in the Institute of Power Transmission and High Voltage Technology at the University of Stuttgart. The authors wishes to thank Prof. Stefan Tenbohlen for providing testing facilities. Technical assistance of Dr. Simon Burow is also greatly appreciated.

VII. References

[1] S.A. Boggs, F.Y. Chu, N. Fujimoto, A. Krenicky, A. Plessl, D. Schlicht, “Disconnect Switch Induced Transients and Trapped Charge in Gas-Insulated Substations,” *IEEE Trans. PAS-101*, October, 1982.

[2] M. Szewczyk, “Multi-spark approach on VFTO modeling in Gas-Insulated Switchgear – Part I: Physical assumptions and model development,” [submitted for publication]

[3] A. Tavakoli, A. Gholami, H. Nouri, M. Negnevitsky, "Comparison between suppressing approaches of Very Fast Transients in Gas-Insulated Substations (GIS)," IEEE Trans. Power Delivery, vol. 28, no 1, pp. 303-310, Jan. 2013.

[4] U. Riechert, M. Bösch, M. Szewczyk, W. Piasecki, J. Smajic, A. Shoory, S. Burow, S. Tenbohlen, “Mitigation of Very Fast Transient Overvoltages in Gas Insulated UHV Substations”, 44th CIGRÉ Session, 2012.

[5] M. Szewczyk, J. Pawłowski, K. Kutorasiński, W. Piasecki, M. Florkowski, U. Straumann, “High Frequency Model of Magnetic Rings for Simulation of VFTO Damping in Gas-Insulated Switchgear with Full-scale Validation,” *IEEE Trans. Power Delivery,* [accepted for publication].

[6] S. Burow, S. Tenbohlen, W. Köhler, J. Smajic, A. Tröger, W. Holaus, "Can ferrite materials or resonant arrangements reduce the amplitudes of VFTO in GIS," in Proc. 2011 17th International Symposium on High Voltage Engineering, Hannover, Germany, 2011.

[7] Y. Guan, G. Yue, W. Chen, Z. Li, W. Liu, “Experimental Research on Suppressing VFTO in GIS by Magnetic Rings,” *IEEE Trans. Power Delivery*, vol. 28, No. 4, pp. 2558-2565, Oct 2013.

[8] M. Szewczyk, K. Kutorasiński, J. Pawłowski, W. Piasecki, M. Florkowski, “Advanced modeling of magnetic cores for damping of high frequency power system transients,” [submitted for publication]

[9] J. He, Y. Guan, W. Liu, W. Chen, Z. Li, "Design Optimization of Ferrite Rings for VFTO Mitigation," IEEE Trans. Power Delivery, 2014 (accepted for publication).

[10] Magnetec GmbH, “Product specification for inductive components,” [Online] (material data sheet). Available: www.magnetec.de, 2015.

[11] S. Burow, U. Straumann, W. Köhler, S. Tenbohlen, “New Methods of Damping Very Fast Transient Overvoltages in Gas-Insulated Switchgear,” *IEEE Trans. Power Delivery*, vol. 29, No. 5, pp. 2332-2339, October 2014.

VIII. Biographies

This article has been accepted for publication in a future issue of this journal, but has not been fully edited. Content may change prior to final publication. Citation information: DOI 10.1109/TPWRD.2016.2524677, IEEE Transactions on Power Delivery

Marcin Szewczyk (M'2012–SM'2014) received his M.Sc. and Ph.D. degrees in Electrical Engineering from Warsaw University of Technology, Warsaw, Poland, in 2000 and 2009 respectively. He was Assistant Professor at Warsaw University of Technology. Since 2010 he is a Researcher with ABB Corporate Research in Cracow, Poland. His research is mainly in the field of power system analyses and advanced simulations, power products, transients analyses and transients mitigation, insulation coordination, 3D modeling and simulations of electromagnetic fields, modeling of magnetic materials for transient analyses.

Dr. Szewczyk is a member of IEEE and Polish Society for Theoretical and Applied Electrical Engineering (ABB Corporate Research, Starowislna 13A, 31-038 Krakow, Poland, E-mail: marcin.szewczyk@pl.abb.com).

Wojciech Piasecki was born in Poland on May 15,1966. He received the M.Sc. degree in electronics from the University of Science and Technology, in Kraków Poland, Poland, and the Ph.D. degree from the Jagiellonian University, Kraków. He has been working for many years in electromagnetic and electrical phenomena, including high-frequency and nonlinear modeling of electrical equipment. Currently, he is a Researcher with the Corporate Research Center in Kraków. His main research concentrates around transient network phenomena analysis.

Mariusz Stosur, received M.Sc. and Ph.D. degrees in the Faculty of Electrical Engineering from the Wroclaw University of Technology, Poland in 1999, 2004 respectively. His research fields of interests include switching phenomenon in vacuum and gaseous medium, power transformers and instrument transformers, power system protection, insulation coordination studies, transients analyses and non-linear modeling and simulations in electrical power engineering. Currently, he is a research scientist at ABB Corporate Research Center in Krakow, Poland.

Marek Florkowski (M'97-SM'08) received the M.S. and Ph.D. degrees in electronics from AGH University of Science and Technology in Kraków in 1990 and 1994, respectively. From 1990 to 1992 he was employed at ABB Corporate Research Center in Baden-Dättwil. In 2009 he obtained habilitation. He is currently responsible for ABB Corporate Research in Krakow, Poland. A member of CIGRE, and APEE. He is chair of the Technical Committee on Diagnostics of the IEEE Dielectrics and Electrical Insulation Society.

Uwe Riechert (M'13) received the Ph.D. degree in electrical engineering on the topic of polymeric-insulated HVDC cables at the Dresden Technical University (TUD), Dresden, Germany, in 2001. Since 1999, he has been with ABB Switzerland, Zurich, Switzerland. He conducted several product development projects [gas-insulated switchgear, generator circuit breakers, and ultra-high voltage (UHV)] and in 2013, he became a Principal Manager. Since 2011, he has been a Project Manager for HVDC substations. Dr. Riechert is a member of DKE, CES, and CIGRE, and leads different CIGRE and CES working and advisory groups.